Course EE5104: Adaptive Control System (Part I)

CA3 Project

Adaptive Control of Angular Positin with Full-State Measurable on the D.C. Motor

Lecturer: **Prof. Lee, Tong Heng**

Author: XU YIMIAN
Student ID: A0295779Y

National University of Singapore

Apr 17, 2025

Contents

List of Tables

List of Figures

Chapter 1

Calibration

1.1 System Setup

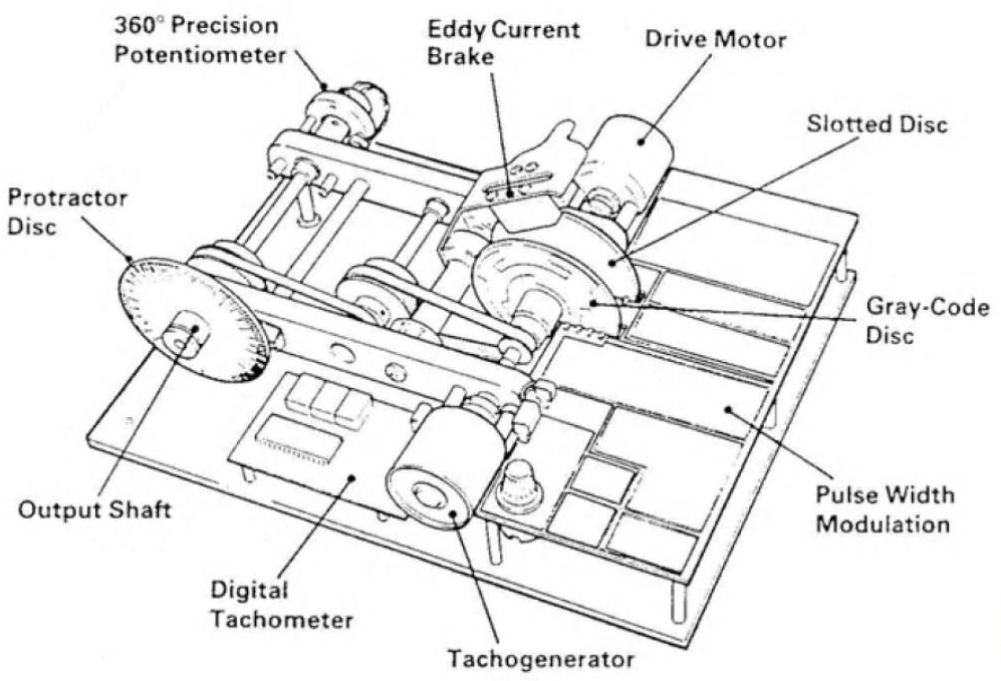

Figure 1.1: D.C Motor

This report presents a simulation-based adaptive control design for a D.C. motor system modeled after the L.J. Electronics D.C. motor apparatus (shown in Fig. 1.1). The dynamic of the system can be approximated to a second order system, with 4 unknown parameters to be obtained (shown in Fig. 1.2). The D.C. motor has angular position (potentiometer) and angular velocity (tachometer) sensors. In order to be able use these for implementing a control system for the motor, the voltage outputs of the sensors need to be calibrated to the actual angular position and angular velocity measurements.

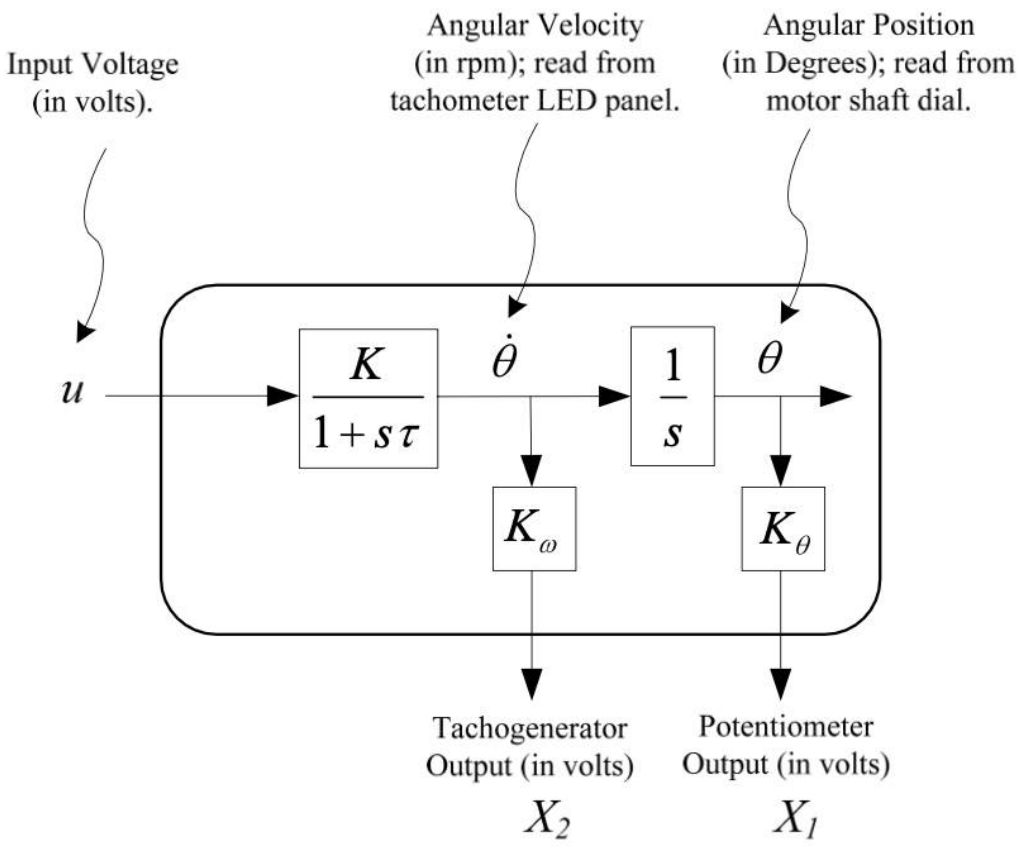

Figure 1.2: Nominal Dynamic Model of Motor

1.2 Calibration of the D.C. motor sensors

Calibration data is shown in Table 1.1 and 1.2. The data is plotted and LS algorithm is applied to obtain the parameter estimations (shown Fig. 1.3 and 1.4). From the LS estimation, we have: $K_\theta = 1.5915\ V/rad$, $K_\omega = 0.1278\ V/rad \cdot s^{-1}$ and $K = 6.1842\ rad \cdot s^{-1}/V$. For purpose of simulation of this motor, it is stated that this apparatus has the values of K = 6.2 $rad \cdot s^{-1}/V$, and $\tau = 0.25$ seconds.

Table 1.1: Calibration Data for Potentiometer Sensor

θ [deg]	θ [rad]	X_1 [V]
−180.00	−3.14	−5.00
−144.00	−2.51	−4.00
−108.00	−1.88	−3.00
−72.00	−1.26	−2.00
−36.00	−0.63	−1.00
0.00	0.00	0.00
36.00	0.63	1.00
72.00	1.26	2.00
108.00	1.88	3.00
144.00	2.51	4.00
180.00	3.14	5.00

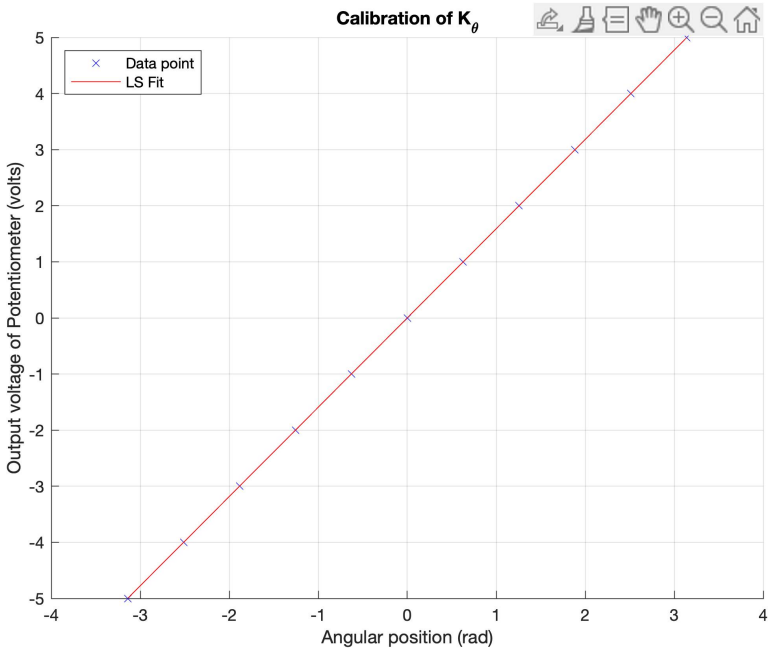

Figure 1.3: Calibration of K_θ

Table 1.2: Calibration Data for Tachogenerator Sensor

u [V]	ω [rpm]	ω [rad/sec]	X_2 [V]
−5.00	−301.00	−31.52	−3.14
−4.00	−237.00	−24.82	−2.51
−3.00	−172.00	−18.01	−1.88
−2.00	−108.00	−11.31	−1.26
−1.00	−45.00	−4.71	−0.63
0.00	0.00	0.00	0.00
1.00	48.00	5.03	0.63
2.00	111.00	11.62	1.26
3.00	175.00	18.33	1.88
4.00	239.00	25.03	2.51
5.00	303.00	31.73	3.14

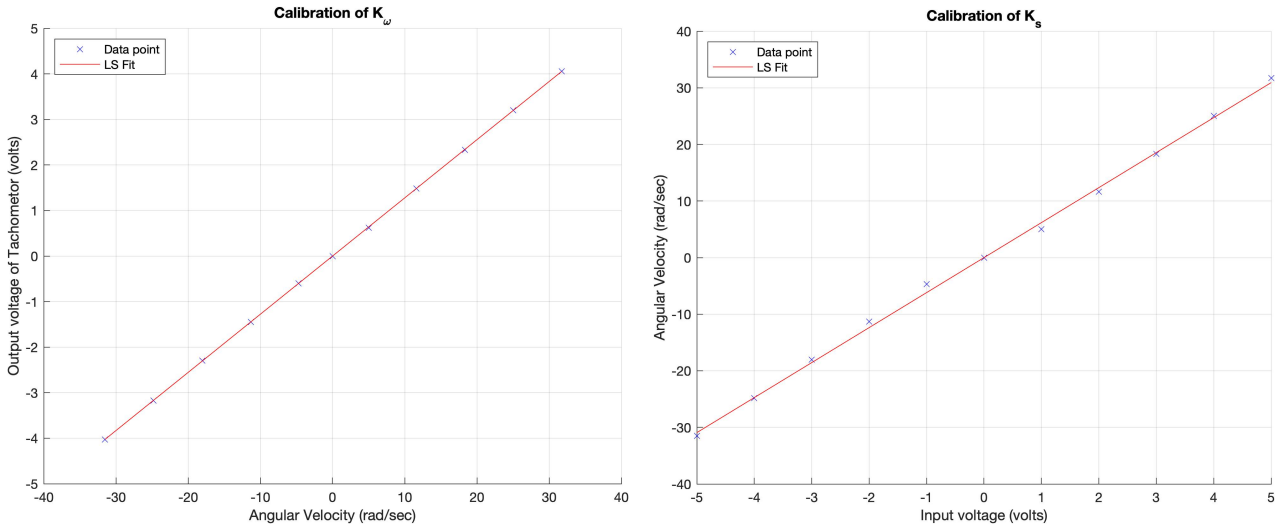

(a) Calibration of K_ω (b) Calibration of K_s

Figure 1.4: Calibration Results

Chapter 2

Adaptive Control Design

To implement adaptive control law design, the actual plant parameters are not required. Dynamic system parameters (K and τ) are for simulation purposes to verify the controller. The adaptive controller can be designed with the following steps:

1. Plant description
2. Reference model
3. Applying matching condition
4. Adaptive control law design

The block diagram of a model reference adaptive system with state-feedback is shown in Fig. 2.1.

2.1 Plant Description

The nominal model of the D.C. motor is a first-order system given by:

$$\dot{\omega}(t) = -\frac{1}{\tau}\omega(t) + \frac{K}{\tau}u(t) \tag{2.1}$$

where:

- $\omega(t)$: Angular velocity (rad/s)
- $u(t)$: Input voltage (V)
- $K = 6.2$: Steady-state gain (rad/s per volt)
- $\tau = 0.25$: Time constant (s)

Sensor outputs are simulated based on calibration:

$$X_1(t) = K_\theta \theta(t) \quad \text{(Position sensor output)} \tag{2.2}$$

$$X_2(t) = K_\omega \omega(t) \quad \text{(Velocity sensor output)} \tag{2.3}$$

The actuator is voltage-limited:

$$|u(t)| \leq 5 \text{ volts} \tag{2.4}$$

Define the state vector $x_p = [\theta \quad \omega]^T$, the state space representation of the plant shown in Fig. 1.2 is formulated as follows:

$$\dot{x}_p = A_p x_p + gbu \tag{2.5}$$

where:

$$A_p = \begin{bmatrix} 0 & 1 \\ 0 & -\frac{1}{\tau} \end{bmatrix}, \quad g = \frac{K}{\tau}, \quad b = \begin{bmatrix} 0 \\ 1 \end{bmatrix} \tag{2.6}$$

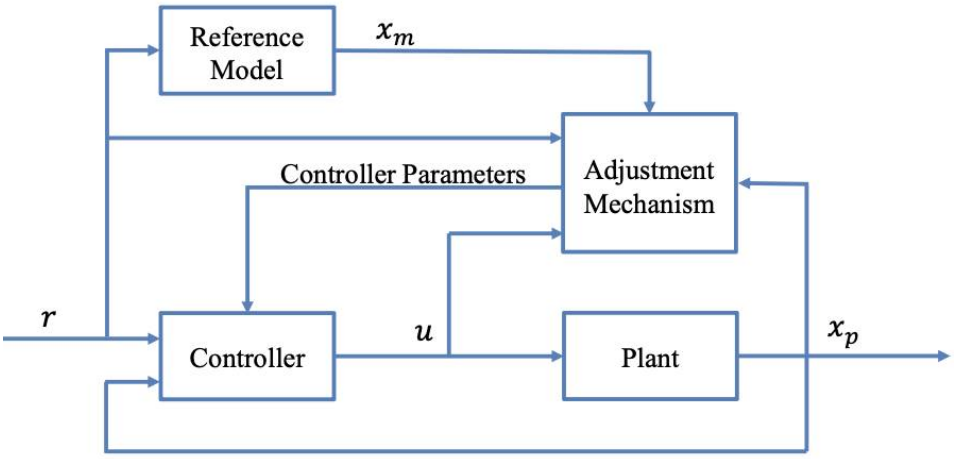

Figure 2.1: Block Diagram

2.2 Reference Model

To apply Model Reference Adaptive Control on the D.C. motor, a 2nd-order reference model is designed. The transfer function of reference model is:

$$H_m(s) = \frac{\omega_m^2}{s^2 + 2\zeta_m \omega_m s + \omega_m^2} \tag{2.7}$$

The state space representation of the reference model can be obtained:

$$\dot{x}_m = A_m x_m + g_m b r \tag{2.8}$$

where:

$$A_m = \begin{bmatrix} 0 & 1 \\ -\omega_m^2 & -2\zeta_m \omega_m \end{bmatrix}, \quad g_m = \omega_m^2 \tag{2.9}$$

2.3 Matching Condition

Consider a control law as follows:

$$u = \theta_x^T x_p + \theta_r r \tag{2.10}$$

Assume that A_p and g in Eq. 2.5 are known. Substitute the control signal described by Eq. 2.10 into Eq. 2.5 to obtain the closed-loop system described as follows:

$$\begin{aligned}\dot{x}_p &= A_p x_p + gb(\theta_x^T x_p + \theta_r r) \\ &= (A_p + gb\theta_x^T)x_p + gb\theta_r r\end{aligned} \tag{2.11}$$

If we choose $\theta_x = \theta_x^*$, $\theta_r = \theta_r^*$, where θ_x^* and θ_r^* are such constant that

$$(A_p + gb\theta_x^{*T}) \equiv A_m, \quad g\theta_r^* \equiv g_m,$$

the closed-loop system would be identical to the reference model in Eq. 2.8. A perfect model-following system is obtained.

2.4 Adaptive Control Law Design

In practice, $\theta_x = \theta_x^*$ and $\theta_r = \theta_r^*$ cannot be calculated since A_p and g are unknown. So we consider making them time-varying gain such that the control law:

$$u(t) = \theta_x(t)^T x_p(t) + \theta_r(t) r(t) \tag{2.12}$$

The closed-loop system dynamics is given in Eq. 2.11. It is equivalent to:

$$\begin{aligned}\dot{x}_p &= \left(A_p + gb\theta_x^T\right) x_p + gb\theta_r r + gb\theta_x^{*T} x_p - gb\theta_x^{*T} x_p + gb\theta_r^{*T} r - gb\theta_r^{*T} r \\ &= \left(A_p + gb\theta_x^{*T}\right) x_p + gb\theta_r^* r + gb\left[(\theta_x^T - \theta_x^{*T})x_p + (\theta_r - \theta_r^*)r\right] \\ &= A_m x_p + g_m b r + gb\left[\psi_x^T x_p + \psi_r r\right]\end{aligned} \tag{2.13}$$

where $\psi_x = \theta_x - \theta_x^*$, $\psi_r = \theta_r - \theta_r^*$.

By applying some adaptive law to the control gain, we want to make the state error $e = x_p - x_m$ converge to 0.

Subtract Eq. 2.8 from Eq. 2.13 to obtain $\dot{e}$ as follows. It shows that $\dot{e} = 0$ when $e = 0$, $\psi_x = 0$ and $\psi_r = 0$.

$$\dot{e} = A_m e + gb\left[\psi_x^T x_p + \psi_r r\right] \tag{2.14}$$

Consider a Lyapunov function $V(e, \psi_x, \psi_r)$:

$$V(e, \psi_x, \psi_r) = \frac{1}{2} e^T P e + \frac{1}{2}|g|\psi_x^T \Gamma^{-1} \psi_x + \frac{1}{2}|g|\frac{1}{\gamma}\psi_r^2 \tag{2.15}$$

where P is the solution to the Lyapunov equation $A_m^T P + P A_m = -Q$ with Q any arbitrarily chosen symmetric positive definite matrix (A_m must be asymptotically stable); Γ is a positive definite diagonal matrix; γ is a positive scalar.

V is a positive definite function: $V = 0$ iff $e = 0$, $\psi_x = 0$ and $\psi_r = 0$; otherwise $V > 0$. $\dot{V}$ can be calculated as follows from Eq. 2.15:

$$\dot{V} = e^T P \dot{e} + |g|\psi_x^T \Gamma^{-1} \dot{\psi}_x + |g|\frac{1}{\gamma}\psi_r \dot{\psi}_r \tag{2.16}$$

Substitute Eq. 2.14 into Eq. 2.16,

$$\begin{aligned}\dot{V} &= e^T P\left(A_m e + gb\left(\psi_x^T x_p + \psi_r r\right)\right) + |g|\,\psi_x^T \Gamma^{-1}\dot{\psi}_x + |g|\,\frac{1}{\gamma}\psi_r\dot{\psi}_r \\ &= e^T P A_m e + e^T P g b \psi_x^T x_p + e^T P g b \psi_r r + |g|\,\psi_x^T \Gamma^{-1}\dot{\psi}_x + |g|\,\frac{1}{\gamma}\psi_r\dot{\psi}_r \end{aligned} \tag{2.17}$$

Notice that

$$e^T P A_m e = \frac{1}{2}e^T (PA_m + A_m^T P)e = -\frac{1}{2}e^T Q e \tag{2.18}$$

Therefore, Eq. 2.17 becomes:

$$\dot{V} = -\frac{1}{2}e^T Q e + e^T P g b \psi_x^T x_p + |g|\,\psi_x^T \Gamma^{-1}\dot{\psi}_x + e^T P g b \psi_r r + |g|\,\frac{1}{\gamma}\psi_r\dot{\psi}_r \tag{2.19}$$

To cancel out the blue and red color parts shown above, we design the adaptive law as follows:

$$\dot{\psi}_x = \dot{\theta}_x = -\operatorname{sgn}(g)\,\Gamma e^T P b x_p \tag{2.20}$$

$$\dot{\psi}_r = \dot{\theta}_r = -\operatorname{sgn}(g)\,\gamma e^T P b r \tag{2.21}$$

We can see that $\dot{\psi}_x = 0$, $\dot{\psi}_r = 0$ when $e = 0$, together with Eq. 2.14, it is clear that the equilibrium point of the system composed of e, ψ_x and ψ_r. Substitute the adaptive control law into Eq. 2.19, we have:

$$\dot{V} = -\frac{1}{2}e^T Q e \leq 0 \tag{2.22}$$

$\dot{V}$ is negative semidefinite. Therefore, e, ψ_x and ψ_r are globally Lyapunov stable about the equilibrium point 0. From the Lyapunov stability and Eq. 2.14, we can see that $\| \dot{e} \|$ is bounded, so e is a uniformly continuous function for $t \geq t_0$. Since e is uniformly continuous and the integral $\int_{t_0}^{t} \frac{1}{2} e^T Q e\, d\tau$ is bounded, we have: $\lim_{t\to\infty} e = 0$.

The adaptive control law is designed to control the time-varying gains as follows:

$$\begin{bmatrix}\dot{\theta}_x \\ \dot{\theta}_r\end{bmatrix} = -sgn(g)\Gamma \begin{bmatrix}x_p \\ r\end{bmatrix} e^T P b \tag{2.23}$$

where Γ is a 3×3 adaptive gain matrix, $e = x_p - x_m$ is the 2×1 state error vector, and P is the 2×2 symmetric positive definite solution of the Lyapunov equation $A_m^T P + P A_m = -Q$, and Q is any 2×2 symmetric positive definite matrix.

Here the reference model state matrix A_m must be chosen to be a Hurwitz matrix in order for the Lyapunov equation to hold true, which means: $\operatorname{Re}(\lambda_i(A_m)) < 0, \forall i$.

Chapter 3

Simulation

3.1 Plant Parameters

For the reference model, set parameters $\zeta = 0.7$ and $\omega_n = 5$ for the first simulation. This model is chosen as it is highly damp and it has fast settling time of 0.7s.

$$H_m(s) = \frac{25}{s^2 + 7s + 25} \tag{3.1}$$

For the positive definite matrix Q, it is chosen as:

$$Q = \begin{bmatrix} 1 & 0 \\ 0 & 1 \end{bmatrix} \tag{3.2}$$

and the solution of Riccati equation gives us:

$$P = \begin{bmatrix} 1.9971 & 0.0200 \\ 0.0200 & 0.0743 \end{bmatrix} \tag{3.3}$$

For the gain Γ, it is chosen to be a diagram matrix such that each value at the diagonal has its own physical meaning. Each value at the diagonal of Γ is correspond to the weight putting on the respective signal (x_1, x_2, or r). The higher weight says that the signal is more significant than the other and more control effort will be put on it. In this simulation,

$$\Gamma = diag(1,1,1) \tag{3.4}$$

The measurement noise gains are set as 0 at first. In this simulation, a simple MATLAB and Simulink file is written and a square wave of amplitude ± 1 is input to the system. The complete MATLAB and Simulink source codes are included in the last chapter of this report.

3.2 Simulink Simulations

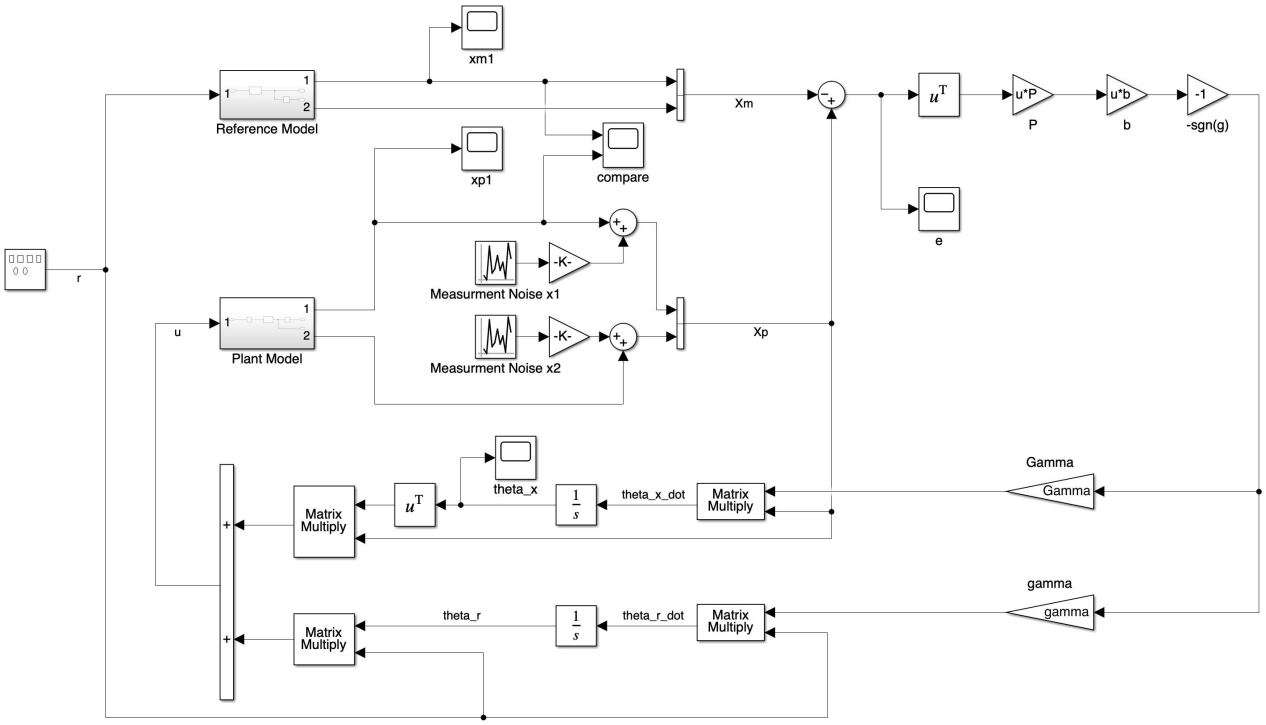

Figure 3.1: Simulink Block Diagram

The Simulink block diagram is shown in Fig. 3.1.

3.3 Investigation of Different Matters

Simulation results are shown in Fig. 3.2 and Fig. 3.3. As we observe from the output plot together with the reference model output, we noticed that the controller has forced the plant output to track the reference signal after the first few period. Looking at the position and velocity error plots, we see that the errors are converging to zero as well. As for the adapted gains shown in Fig. 3.3, since the exact gains can be calculated in the simulation, we see that all the adapted gains, are converging to the exact gains, matching the theoretical derivation shown in the previous chapter.

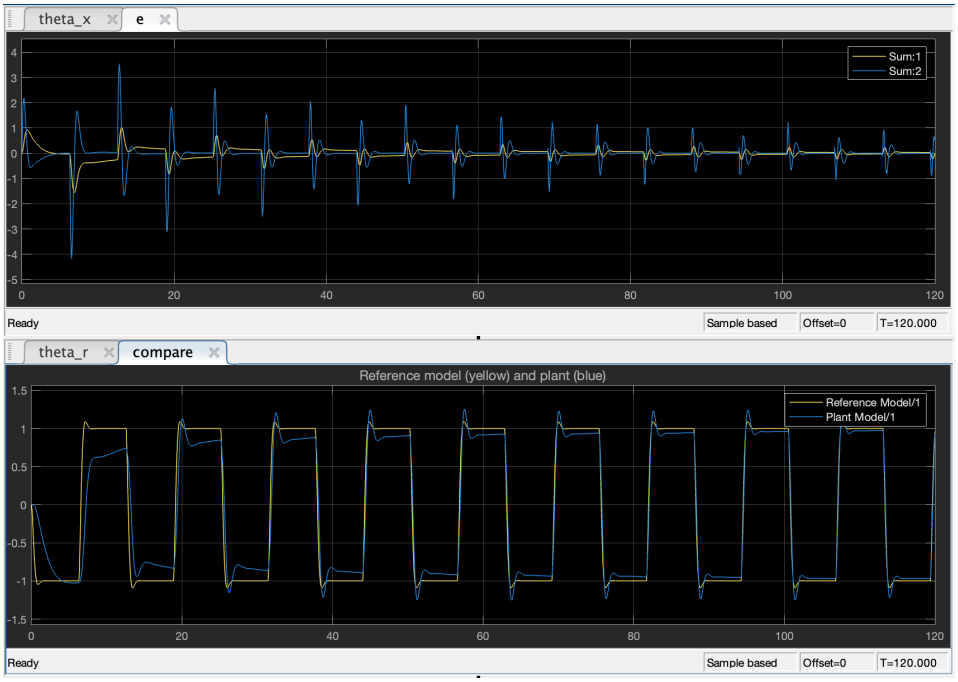

Figure 3.2: Simulation results (Original Setting)

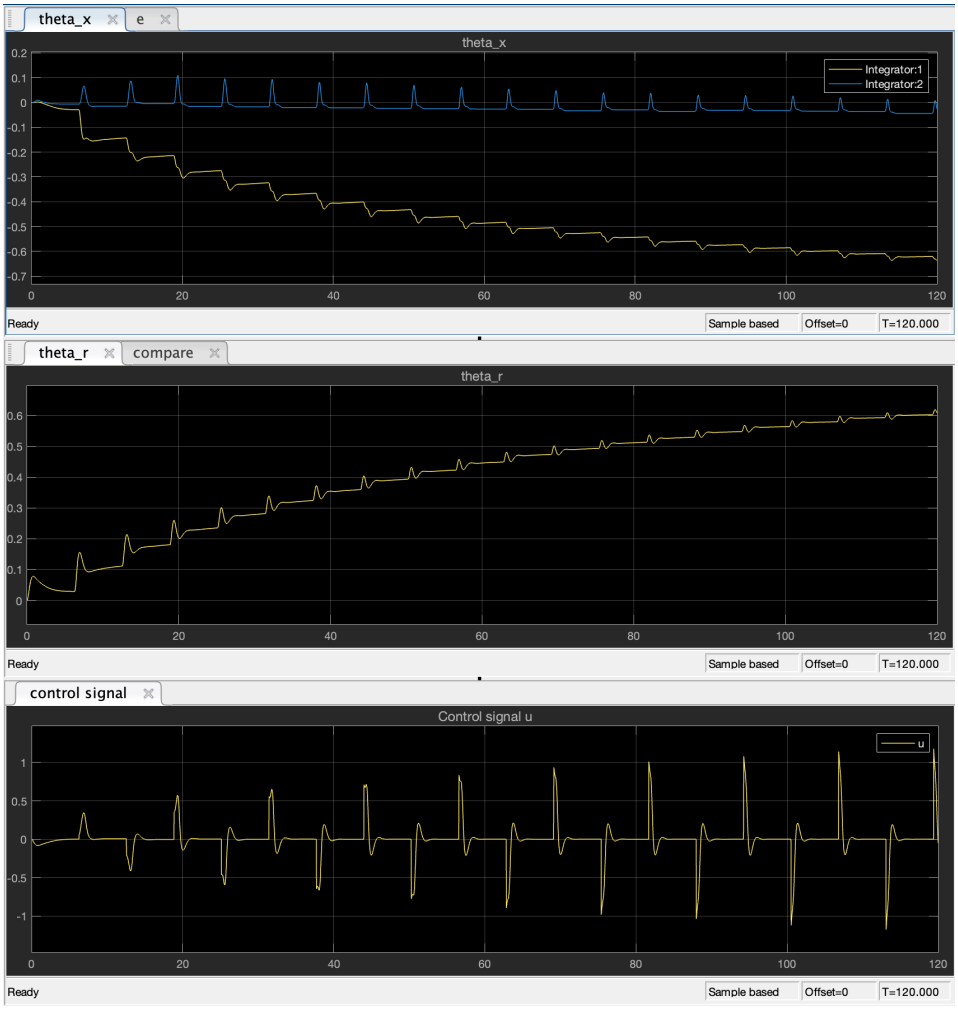

Figure 3.3: Adapted gains (Original Setting)

3.3.1 Different Choices of the Design Parameters

In order to improve the system's response, the gain value, Γ, is replaced by a higher value, with 100 times the original Γ used. Here,

$$\Gamma = diag(100, 100, 100) \tag{3.5}$$

Simulation result is shown in Fig. 3.5 and Fig. 3.4 respectively. The plant managed to track the reference model almost perfectly after the first period (20 seconds). As we know that Γ determines the converge rate of the adapted gains, the higher Γ is, the faster the gains converge to the exact value (shown in Fig. 3.4), and thus the faster the output plant meets the reference model. However, higher control signal is needed in order to force the system to track the reference model.

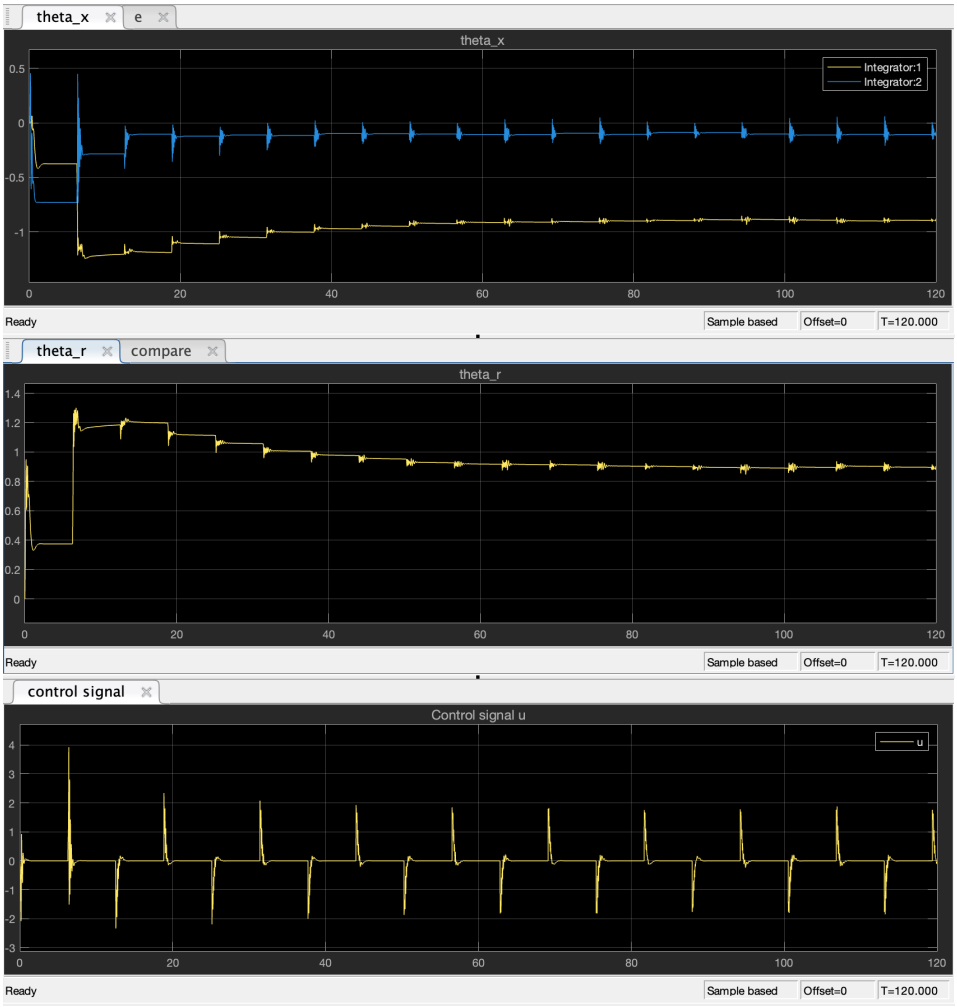

Figure 3.4: Adapted gains ($\Gamma = \text{diag}(100, 100, 100)$)

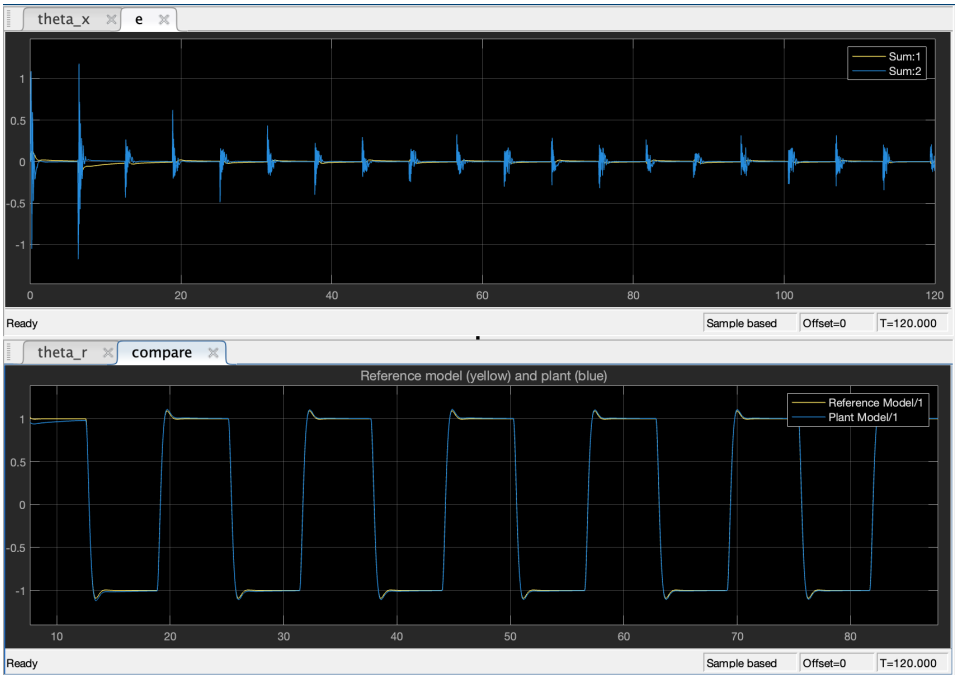

Figure 3.5: Simulation results ($\Gamma = \text{diag}(100, 100, 100)$)

Another approach to reduce the control effort of the system at the same time maintaining the system response, is to choose different adaptive rate for different signal. In this case, since the velocity of the motor is not a control object in the project, we assign the following values to Γ

$$\Gamma = diag(100, 1, 50) \tag{3.6}$$

The results are shown in Fig. 3.6 and Fig. 3.7. We see the response of the system is similar to the previous, but lower control effort is needed to control the system. From the angular velocity error plot (Fig. 3.6 blue line), we see that the velocity error is larger, but it does not affect the system output significantly.

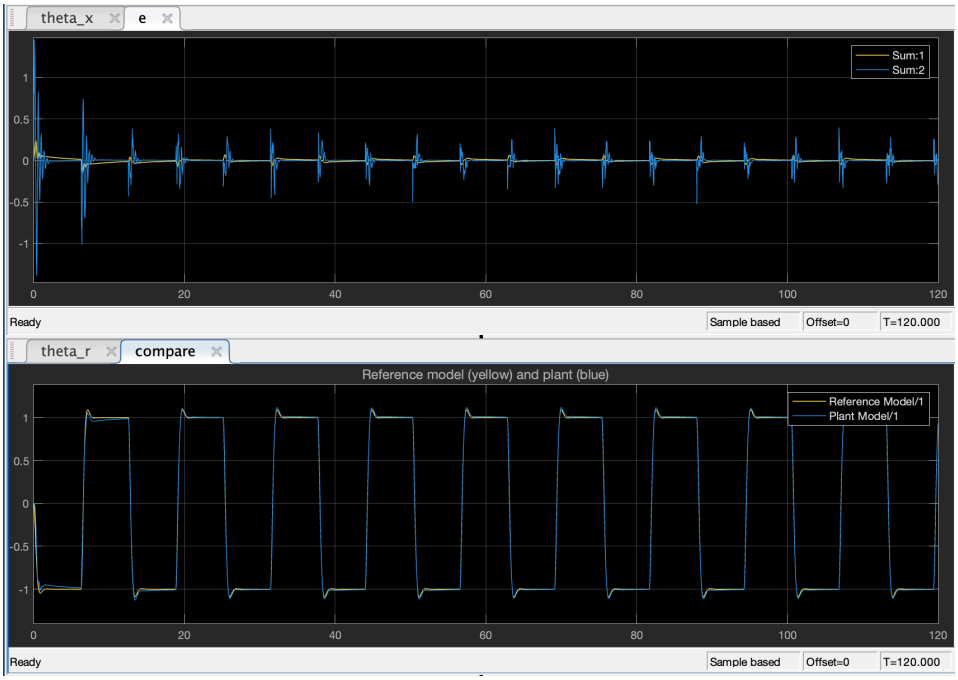

Figure 3.6: Simulation results ($\Gamma = \text{diag}(100, 1, 50)$)

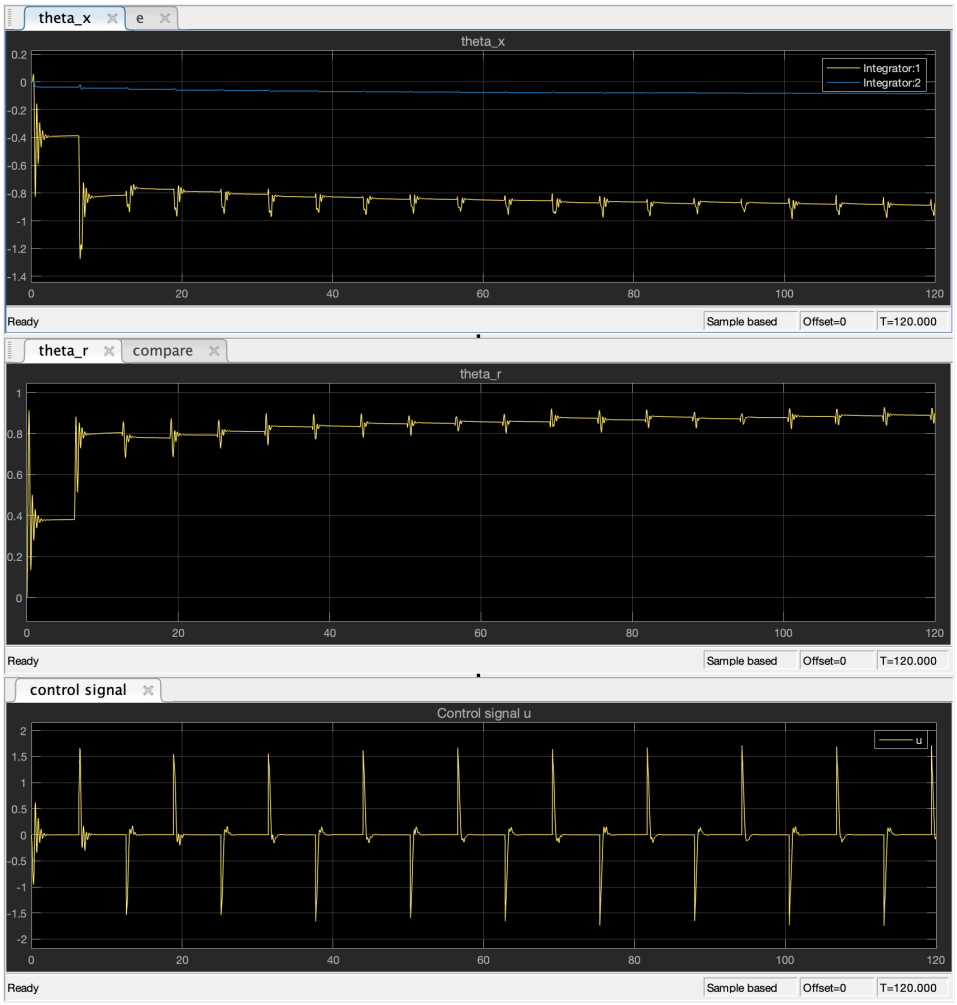

Figure 3.7: Adapted gains ($\Gamma = \text{diag}(100, 1, 50)$)

From $\dot{V} = -e^T Qe$, we see that the higher value of Q leads to a faster rate of convergence of the Lyapunov function, which is the sum of weighted squared errors. In other words, the higher value of Q, the faster the errors converge to zero. Here, we choose Q as:

$$Q = \begin{bmatrix} 50 & 0 \\ 0 & 50 \end{bmatrix} \tag{3.7}$$

Simulation results are shown in Fig. 3.8 and Fig. 3.9. As compared to original setting, we see that the response is much better, as the errors of the system are smaller. However, the more control effort is required to control the system as the values of Q become larger, which is similar to the Γ values.

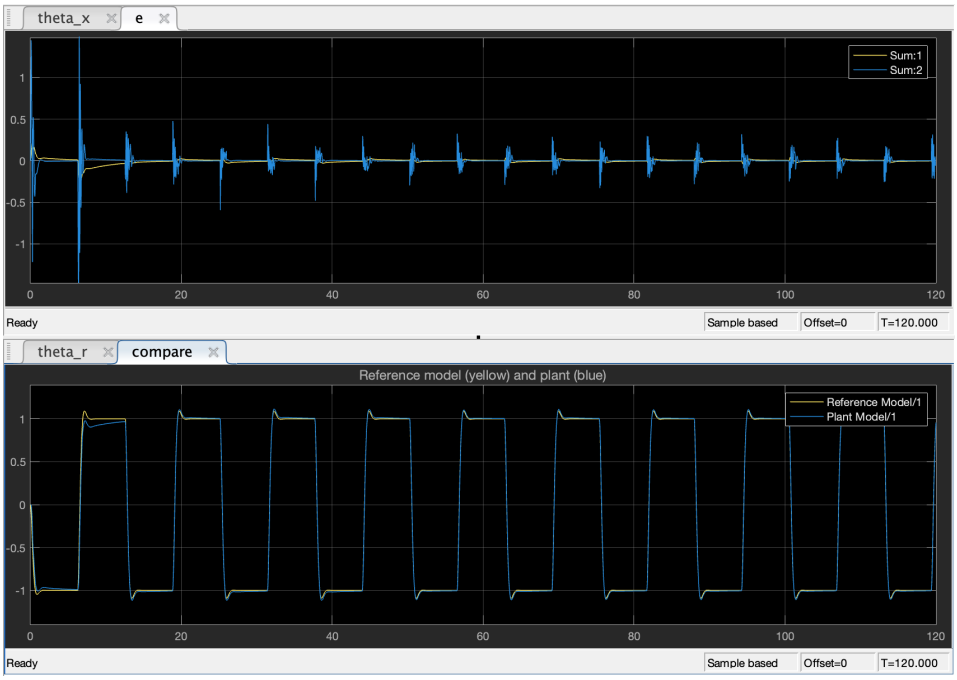

Figure 3.8: Simulation results (Different Q)

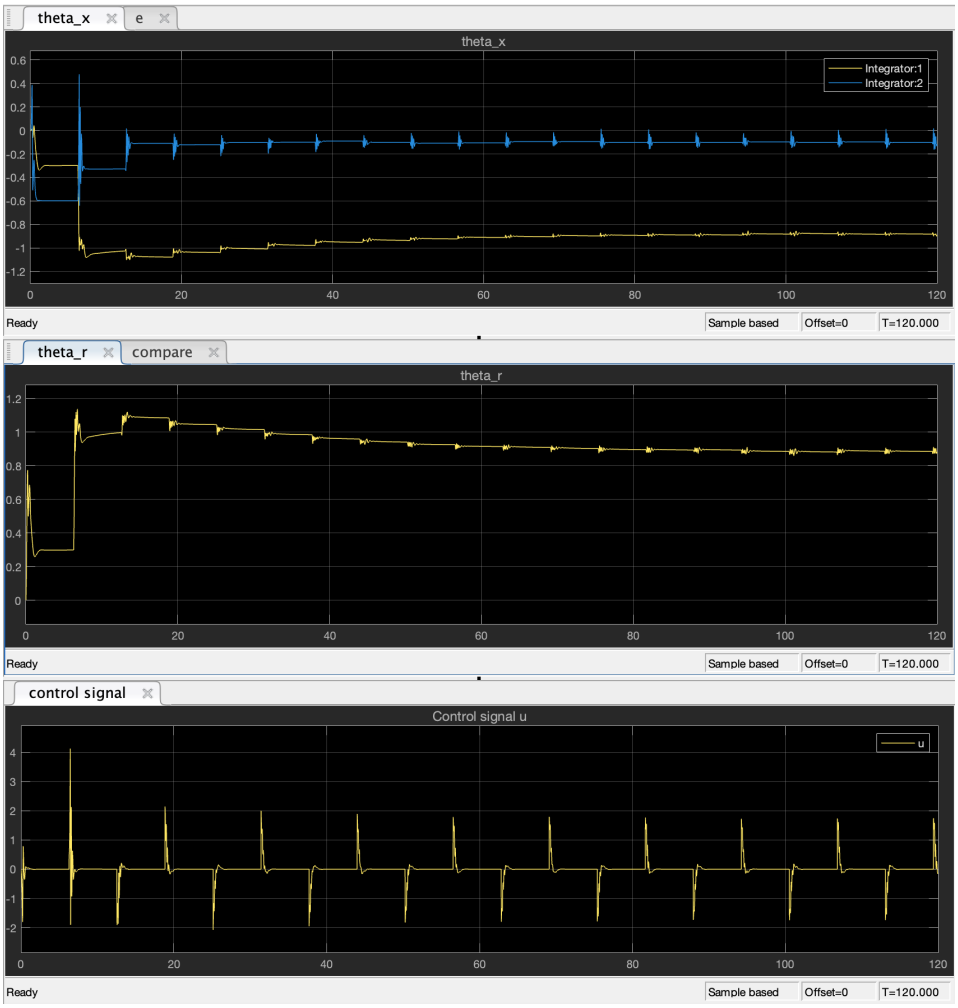

Figure 3.9: Adapted gains (Different Q)

3.3.2 Reference Model State Matrix

In the baseline configuration, the reference model was defined with a natural frequency $\omega_n = 5$ and damping ratio $\zeta = 0.7$, resulting in moderate-speed, underdamped dynamics. To evaluate the impact of the reference model dynamics on the tracking performance, two parameter sets are tested:

1. A model with very low damping ratio ($\zeta = 0.1$) and low natural frequency ($\omega = 3$);
2. A critically damped system ($\zeta = 1$) and higher natural frequency ($\omega = 10$).

Simulation results are shown in Fig. 3.10 to Fig. 3.13. As seen from the plots, the output plants track the first reference model fairly good. It shows that the Γ value here is able to provide a good response to the system. In contrast, the second modified configuration adopted $\omega_n = 10$ and $\zeta = 1.0$, representing a critically damped but significantly faster system. Simulation results show that the plant exhibited inferior tracking performance under the faster model. This degradation is attributed to the limited bandwidth of the actual plant, which could not follow the rapid transitions of the high-speed reference trajectory. This indicates higher values of Γ or Q are required to track the high-frequency reference model.

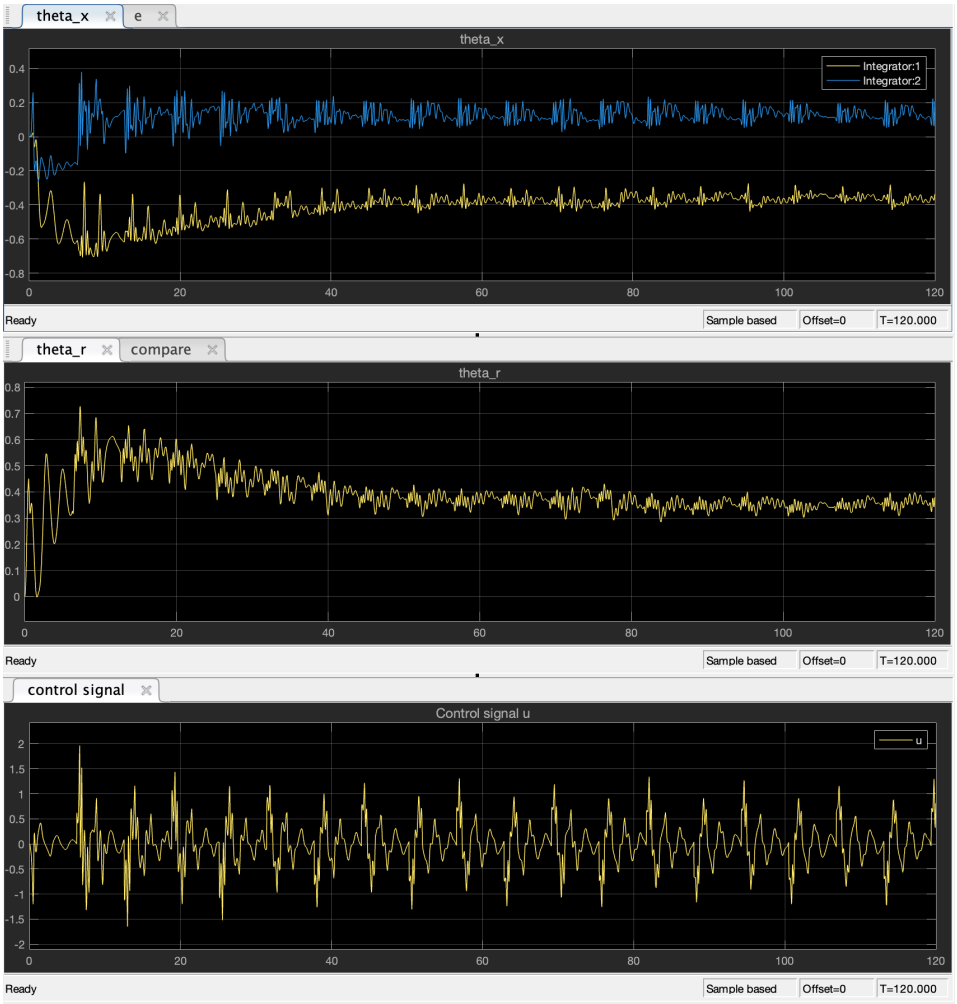

Figure 3.10: Adapted gains ($\zeta = 0.1, \omega = 3$)

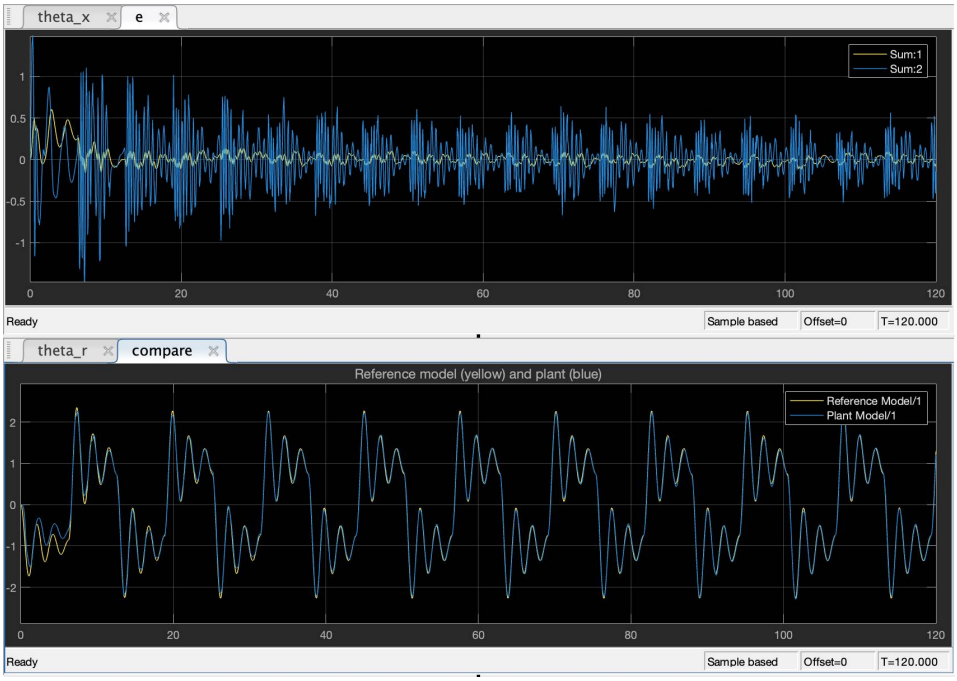

Figure 3.11: Simulation results ($\zeta = 0.1, \omega = 3$)

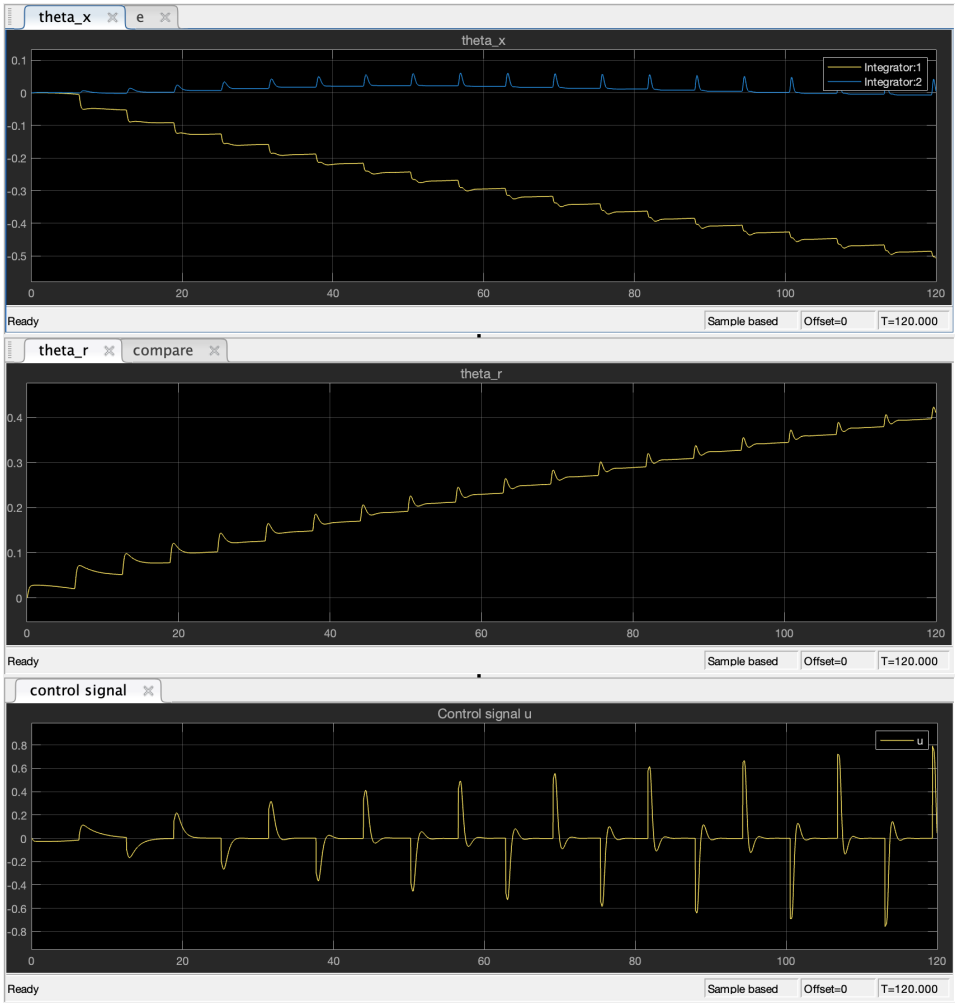

Figure 3.12: Adapted gains ($\zeta = 1, \omega = 10$)

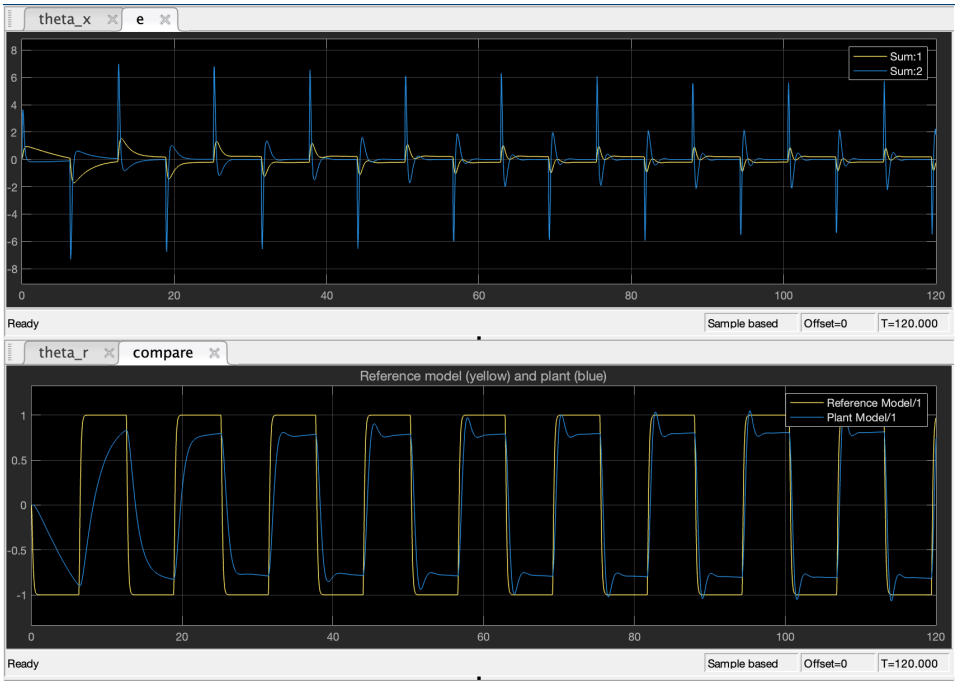

Figure 3.13: Simulation results ($\zeta = 1, \omega = 10$)

3.3.3 Effect of Possible Realistic Noise in the Measurements

To evaluate the robustness of the adaptive control scheme under noisy measurement conditions, a measurement noise signal was introduced into the simulation. Specifically, two normalized random signals were scaled by a gain of 0.1 to limit amplitude and then superimposed onto the measured state variables before being fed into the controller.

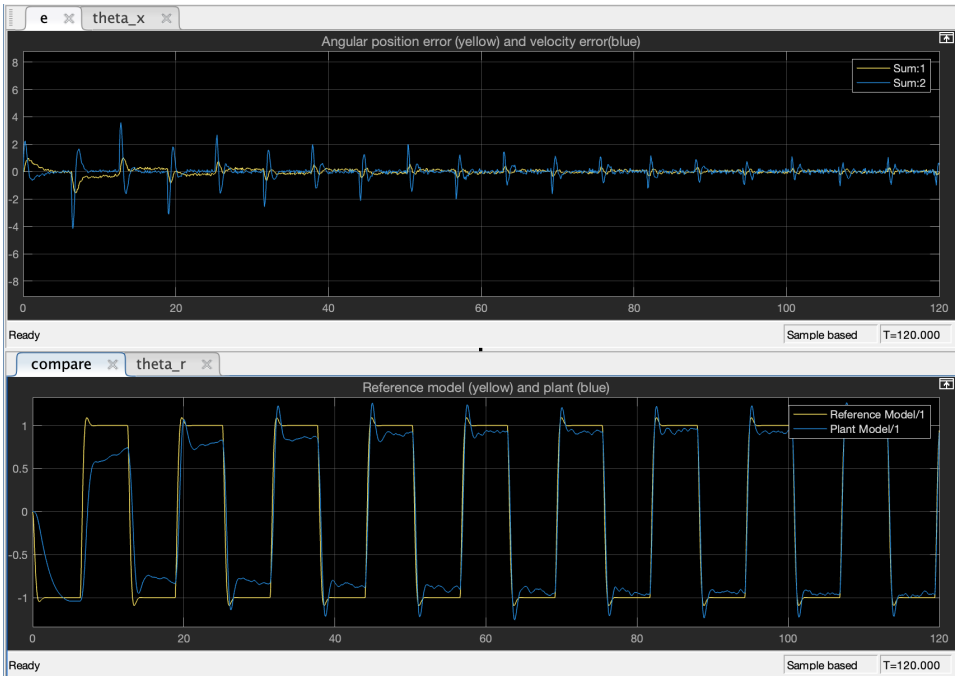

Figure 3.14: Simulation results (Measurement Noise)

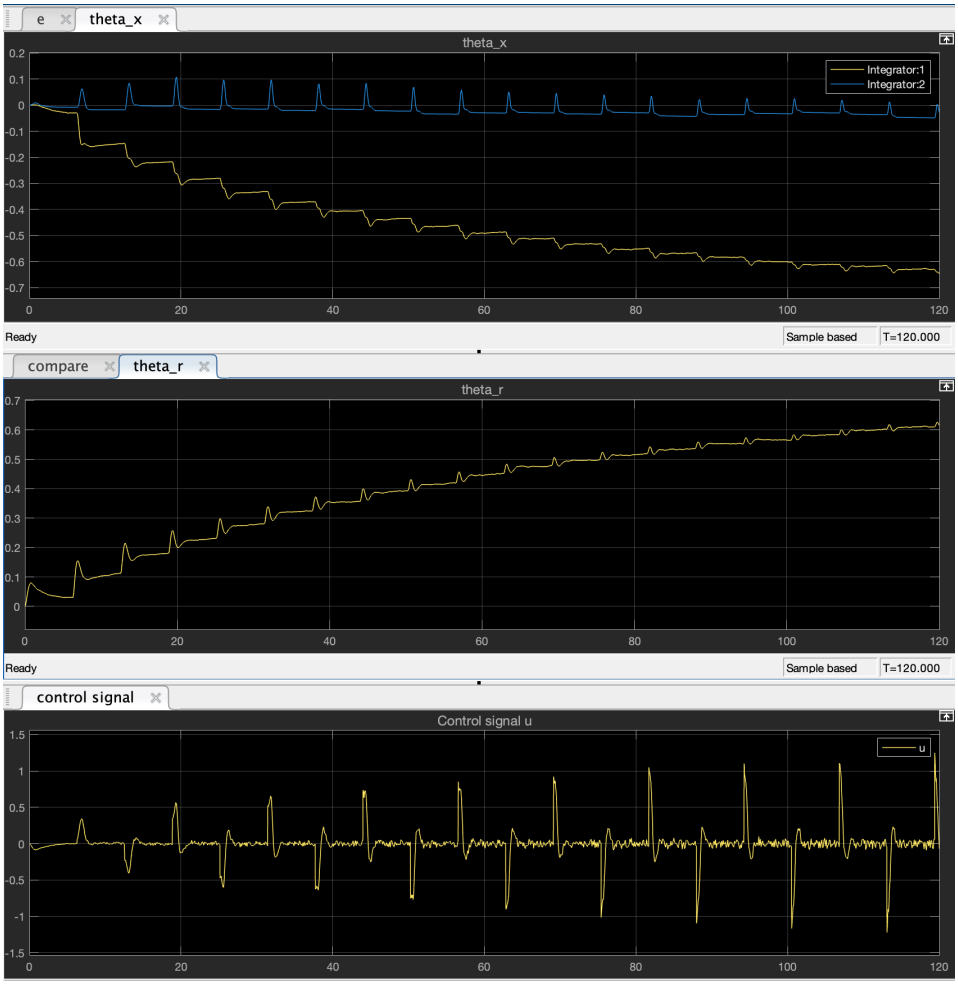

Figure 3.15: Adapted gains (Measurement Noise)

The simulation results are shown in Fig. 3.14 and Fig. 3.15. The plant output exhibited visible fluctuations due to the injected noise. Although the adaptive controller continued to maintain overall stability and convergence, the presence of noise resulted in a noisier control input and slight deviations from the reference model trajectory. It shows the sensitivity of adaptive controllers to measurement noise, as the adaptation law relies directly on error signals computed from noisy measurements.

3.3.4 Different Reference Command Signal r(t)

To assess how different types of reference command signals affect the system's tracking performance, simulations were conducted using various forms of $r(t)$, including sinusoidal signals, and sawtooth waveforms, under the same original parameters.

The simulation results (shown in Fig. 3.16 to Fig. 3.19), reveal that the system's ability to track the reference signal is highly dependent on the signal's frequency content and continuity.

In the previous simulation with a square wave input, the plant struggled to follow the sharp transitions, and even after 120 s, it did not fully converge to the reference. This is due to the discontinuous nature of the square wave, which introduces high-frequency components that challenge the response speed of the plant. In contrast, with a sinusoidal reference, the plant achieved accurate tracking after around 60 s. The continuous and smooth variation of the sine wave results in a more manageable trajectory for the adaptive controller and the plant, allowing better convergence.

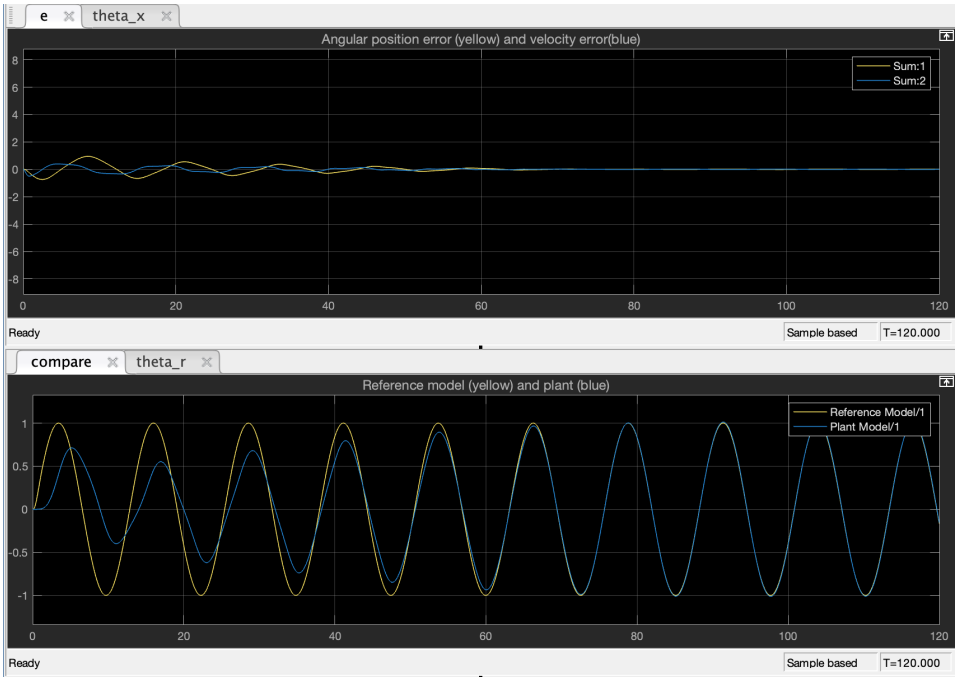

Figure 3.16: Simulation results (Original Setting)

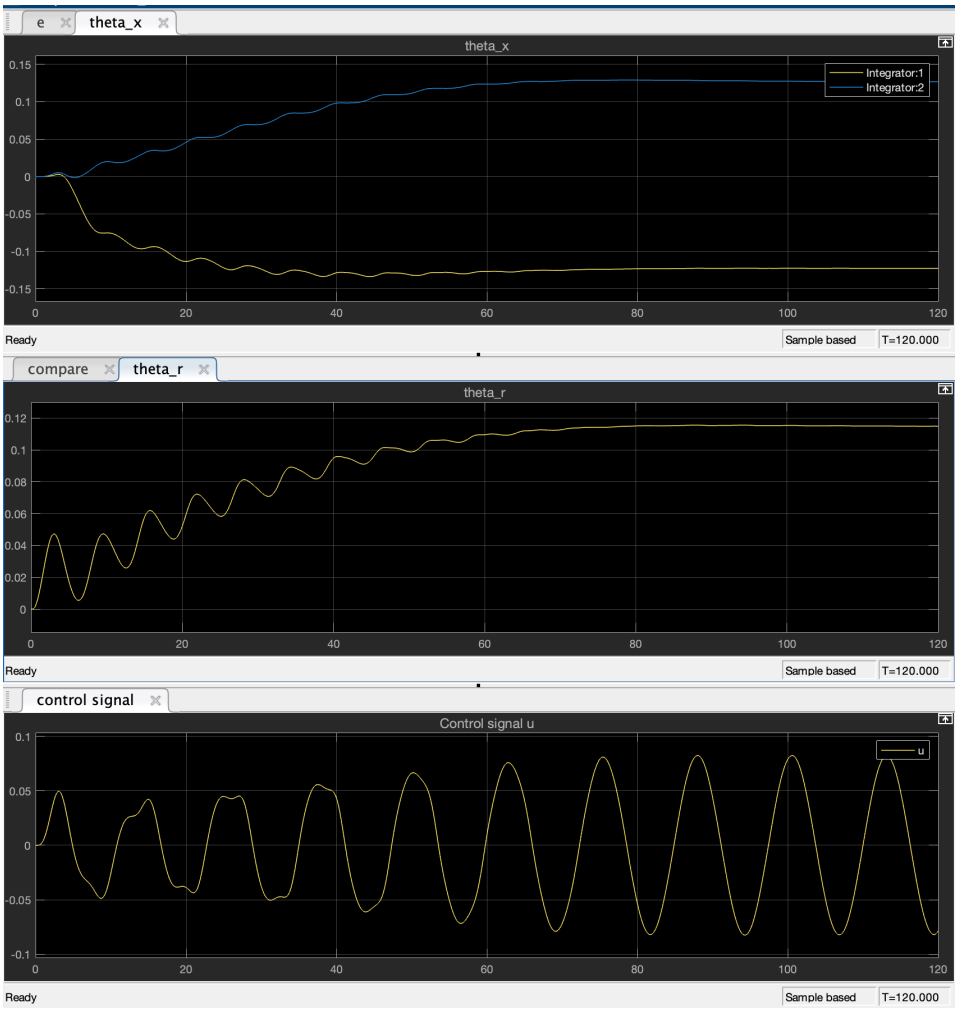

Figure 3.17: Adapted gains (Original Setting)

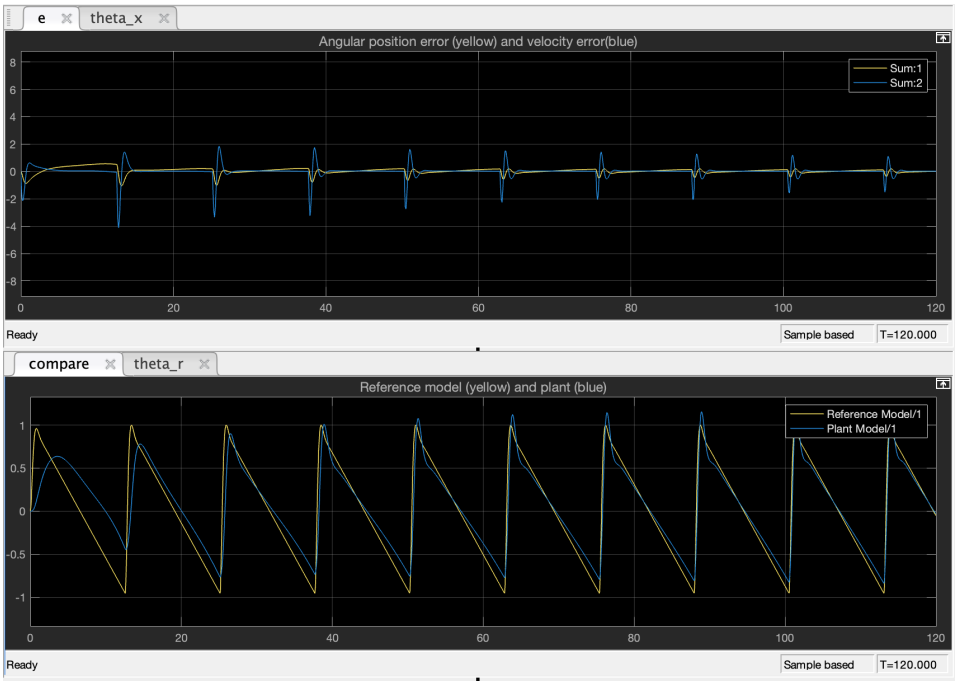

Figure 3.18: Simulation results (Original Setting)

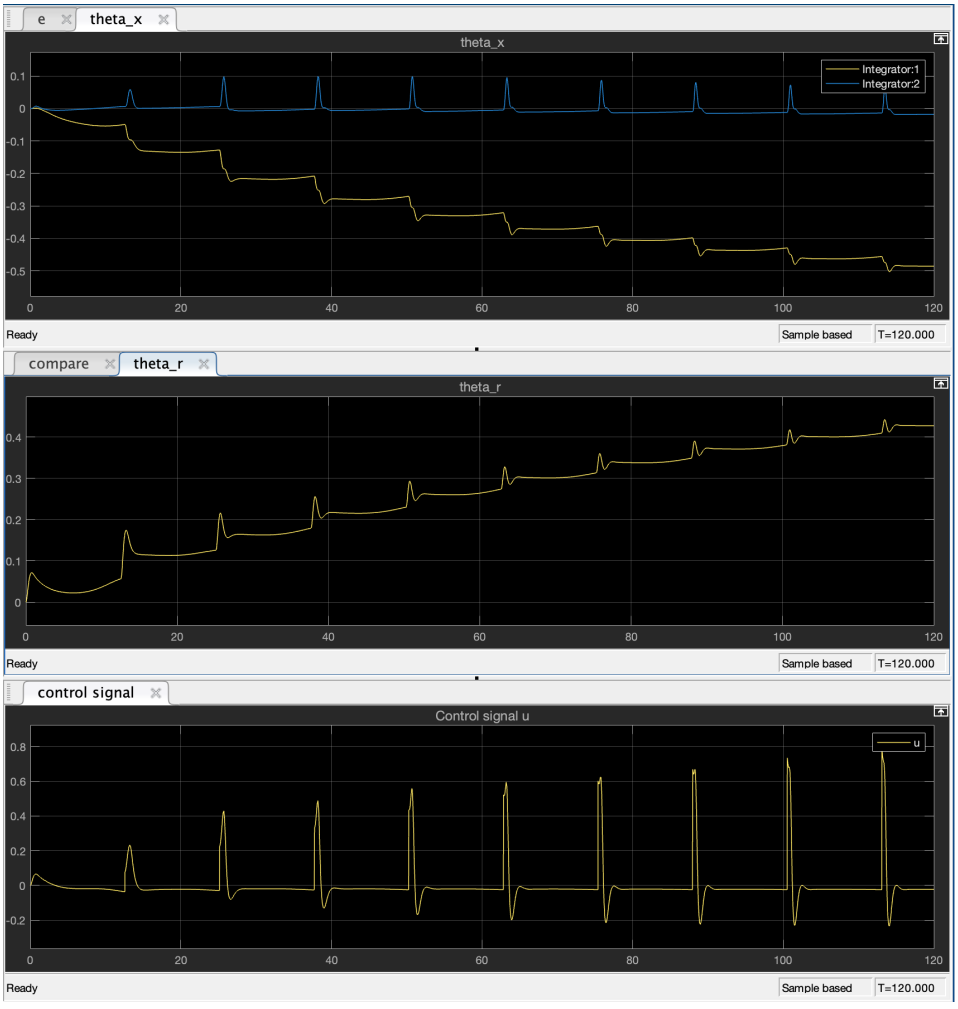

Figure 3.19: Adapted gains (Original Setting)

The tracking performance under a sawtooth wave was comparable to that of the square wave, with similarly poor convergence, especially during abrupt rising and falling edges.

These observations highlight that while the adaptive controller can achieve convergence under smooth and continuous reference trajectories, it becomes less effective when tracking discontinuous or fast-changing inputs. This suggests that for systems with limited bandwidth or slower plant dynamics, smooth reference signals are more appropriate if rapid convergence is desired.

Chapter 4

Code

Task 1: Calibration

```
%% System dynamics and adaptive control:
% Parameters
K = 6.2; tau = 0.25;
Am = [0 1; -4 -2]; Bm = [0; 4];
Gamma = 10*eye(2);

% Simulation time
tspan = [0 10]; x0 = [0; 0]; xm0 = [0; 0]; theta0 = [0; 0];

[t, X] = ode45(@(t,X) adaptive_dc_motor(t, X, Am, Bm, Gamma, K, tau), tspan, [x0; xm0; theta0
    ]);

% Extract states
x = X(:,1:2); xm = X(:,3:4); theta = X(:,5:6);

% Plot
figure;
subplot(2,1,1); plot(t, x(:,1), t, xm(:,1)); legend('Position', 'Reference');
title('Position Tracking');
subplot(2,1,2); plot(t, x(:,2), t, xm(:,2)); legend('Velocity', 'Reference');
title('Velocity Tracking');


%%ODE file: adaptive\_dc\_motor.m
function dXdt = adaptive_dc_motor(t, X, Am, Bm, Gamma, K, tau)
    x = X(1:2); xm = X(3:4); theta = X(5:6);
    r = sin(2*pi*t);
    u = theta' * x;
    u = max(min(u, 5), -5);
    dx = [x(2); (-1/tau)*x(2) + (K/tau)*u];
    dxm = Am * xm + Bm * r;
    e = x - xm;
    dtheta = -Gamma * x * (e' * [0; 1]);
    dXdt = [dx; dxm; dtheta];
end
```

Task 2: Simulation Parameters (Original Settings)

```
%Plant Param
K = 6.2;
tau = 0.25;

%Reference Model Params
C = 0.7;
w = 10;

Am = [0 1;-w^2 -2*C*w];
gm = [0;w^2];

```

```
%Gamma and gamma
Gamma = [100 0;0 1];
gamma = 100;

% Lyapunov
Q=[100 0; 0 1];
b = [0;1];
P = lyap(Am', Q);
fprintf('The solution to the Lyapunov equation is: \n')
disp(P)

%Measurement Noise
noise_gain_x1 = 0;
noise_gain_x2 = 0;
----------------------------------------
The solution to the Lyapunov equation is:
   14.1429    0.5000
    0.5000    0.0714
```